



Low-temperature large reversible magnetocaloric effects of ErNi $1-x$ Cu x Al ($x = 0.2, 0.5, 0.8$) intermetallic compounds

L. C. Wang, Q. Y. Dong, J. Lu, X. P. Shao, Z. J. Mo, Z. Y. Xu, J. R. Sun, F. X. Hu, and B. G. Shen

Citation: [Journal of Applied Physics](#) **114**, 213907 (2013); doi: 10.1063/1.4838040

View online: <http://dx.doi.org/10.1063/1.4838040>

View Table of Contents: <http://scitation.aip.org/content/aip/journal/jap/114/21?ver=pdfcov>

Published by the [AIP Publishing](#)



Re-register for Table of Content Alerts

Create a profile.



Sign up today!



Low-temperature large reversible magnetocaloric effects of $\text{ErNi}_{1-x}\text{Cu}_x\text{Al}$ ($x = 0.2, 0.5, 0.8$) intermetallic compounds

L. C. Wang,¹ Q. Y. Dong,² J. Lu,¹ X. P. Shao,¹ Z. J. Mo,³ Z. Y. Xu,¹ J. R. Sun,¹ F. X. Hu,¹ and B. G. Shen^{1,a)}

¹State Key Laboratory for Magnetism, Institute of Physics, Chinese Academy of Sciences, Beijing 100190, China

²Department of Physics, Capital Normal University, Beijing 100048, China

³School of material Science and Engineering, Hebei University of Technology, Tianjin 300401, China

(Received 8 November 2013; accepted 15 November 2013; published online 5 December 2013)

The magnetic properties and magnetocaloric effects of the $\text{ErNi}_{1-x}\text{Cu}_x\text{Al}$ ($x = 0.2, 0.5, 0.8$) compounds have been studied. The sample with $x = 0.2$ is found to be antiferromagnetic below the Néel temperature of $T_N = 4.6$ K, while the sample $x = 0.5$ is simply ferromagnetic with a Curie temperature of $T_C = 5.8$ K. In contrast, the sample $x = 0.8$ exhibits a short-range magnetic order, as revealed by AC magnetic measurements, and the transition temperature is 5.5 K. Large magnetic entropy change (ΔS) without hysteresis losses has been observed around the transition temperature for all the samples. The ΔS displays a peak between 4 K and 10 K, and the maximal values of ΔS are -22.6 , -25.9 , and -24.8 J/kg K for the field changes of 0-5 T, corresponding to the compositions of $x = 0.2$, $x = 0.5$, and $x = 0.8$, respectively. The large ΔS value as well as no hysteresis loss indicate that $\text{ErNi}_{1-x}\text{Cu}_x\text{Al}$ can be alternative candidates for magnetic refrigerant working at low temperature (<10 K). © 2013 AIP Publishing LLC. [<http://dx.doi.org/10.1063/1.4838040>]

I. INTRODUCTION

Nowadays, people around the world all have strong endorsement of the environmental issues, and a great many measures have been taken to cope with the greenhouse effect. New technologies can quicken the pace to meet the challenge. Magnetocaloric effect (MCE) was first discovered by Warburg in 1881. Magnetic refrigeration based on this effect is a promising technique for its characteristics of high energy-efficiency and being eco-friendly, especially compared with the traditional common gas-compression refrigeration technique.¹⁻⁴ The isothermal magnetic entropy change and the adiabatic temperature change arising from the application (removal) of a magnetic field to (from) a system with magnetic degree of freedom are two important parameters to characterize the MCE of the materials.¹⁻⁸ The practical application of this technique suffers from the limitation of efficient magnetic materials. Generally speaking, the first-order phase transition yields an intensive and sharp magnetocaloric peak while the second-order phase transition produces a broader but less intensive peak. Up to now, much effort has been devoted to the fabrication of various single-phase materials with a high ΔS peak,⁸⁻¹⁰ or composite material formed by several materials with different transition temperatures to get a wide working temperature span. Theoretical studies was also made for the exploration of efficient MCE materials.¹¹

Among the RTX compounds ($R =$ rare-earth metal, $T =$ transition metal, and $X =$ p-metal), $R\text{NiAl}$ and $RCu\text{Al}$ ones crystallizing in the same hexagonal ZrNiAl -type

structures are most extensively studied. In recent years, there have been some investigations focusing on the doping at the R site and the T site. Their derivatives $R\text{Ni}_{1-x}\text{Cu}_x\text{Al}$ compounds also belong to the RTX family,¹²⁻²³ but their magnetic orderings are quite complex.²⁰⁻²³ Although ferromagnetic (FM) orders are found mostly in the $RCu\text{Al}$ compounds, the orders in $R\text{NiAl}$ ones are very complex. The antiferromagnetic (AFM) ordered moments within ab -basal plane were found in PrNiAl , NdNiAl , and ErNiAl , while AFM moments were detected along the c -axis in TbNiAl . There sometimes exists an AFM component within the basal plane but it is accompanied by a stronger FM component along c -axis resulting in a canted magnetic structure, where the moments are oriented with quite big angle from the basal plane in HoNiAl and DyNiAl .¹⁶⁻¹⁸ For the $\text{ErNi}_{1-x}\text{Cu}_x\text{Al}$ compounds, the magnetic property undergoes a very complex variation with the change of the Cu content. The compound is found to be AFM in the a - b basal plane when $x \leq 0.4$ and FM when $x = 0.5$. Signatures of short-range order (SRO) was captured for the compounds with $x = 0.6$ - 0.8 .²² The complex magnetic behaviors in this type of pseudoternaries have been interpreted based on the RKKY interaction.^{23,24} In this paper, we studied the magnetic and MCE properties of three typical constituents, i.e., $\text{ErNi}_{1-x}\text{Cu}_x\text{Al}$ ($x = 0.2, 0.5, 0.8$) with different magnetic characteristics. Large ΔS values and excellent reversibility for magnetic cycling have been observed.

II. EXPERIMENTAL DETAILS

The $\text{ErNi}_{1-x}\text{Cu}_x\text{Al}$ samples were synthesized by arc melting the starting materials (Er, Cu, Ni, and Al) in stoichiometric amounts in a water-cooled copper crucible under the

^{a)}Author to whom correspondence should be addressed. Electronic mail: shenbg@aphy.iphy.ac.cn

protection of high-purity argon atmosphere. The purities of the constituent metals are all better than 99.9 wt. %. 2 at. % excessive Er was used to compensate for the weight loss due to the evaporation during the arc melting. The samples were turned over and remelted for several times to ensure their homogeneity. The obtained ingots were sealed in a vacuum quartz tube and annealed at 973 K for 30 days. The samples were named after their compositions, that is, the $x=0.2$, $x=0.5$, and $x=0.8$ samples. Lattice parameter and phase composition were determined by powder X-ray diffractometer using Cu $K\alpha$ radiation. The DC magnetic measurements were carried out on a commercial superconducting quantum interference device magnetometer (SQUID, Quantum Design). The AC magnetic measurement was performed on the physical property measure system (PPMS, Quantum Design) at various frequencies.

III. RESULTS AND DISCUSSION

The refined standard θ - 2θ powder X-ray diffraction spectrum indicated that the $\text{ErNi}_{1-x}\text{Cu}_x\text{Al}$ compounds crystallized in the hexagonal ZrNiAl -type structure (space group $P\bar{6}2m$, No. 189) without secondary phases, as previously reported.²² Figures 1(a)–1(c) show the temperature-dependent magnetizations (M - T) of the $x=0.2$, $x=0.5$, and $x=0.8$ compounds,

respectively, measured in the zero-field cooling (ZFC) and field-cooling (FC) modes. Both the ZFC and FC curves in Fig. 1(a) exhibit a peak at $T_N=4.6$ K, arising from the AFM to paramagnetic (PM) state transition with as it has been reported by neutron diffraction analysis.²² Fig. 1(b) indicates an FM to PM transition at $T_C=5.8$ K for $x=0.5$. As shown in Fig. 1(c), a quasi Curie-like magnetic transition occurs at $T_{trs}=5.5$ K for $x=0.8$, which is a signature for the presence of SRO as will be confirmed by the following AC susceptibility analysis. It should be pointed out that the magnetic transition temperatures observed in this paper are lower than those of the non-doped ErNiAl ($T_N=6.2$ K) and ErCuAl ($T_C=6.8$ K). Not come singly but in pairs, the ordering temperatures (T_{ord}) of $\text{ErNi}_{1-x}\text{Cu}_x\text{Al}$ reported in Ref. 22 are all lower than those of ErNiAl and ErCuAl . We should keep in mind that ErNiAl shows an AFM order lying within the a - b basal plane while ErCuAl ordered ferromagnetically along the c -axis. It has been reported in Ref. 22 that the lattice parameter c increases monotonically with the increasing of Cu concentration if the sample is FM. This in turn causes an increase of the distance between the two magnetic planes (with Er atoms and part of transition metal atoms) separated by the non-magnetic layer consisting of Al atoms and the other part of transition metal atoms, which may lead to a change of the FM coupling along the c -axis. After a careful examination of the lattice

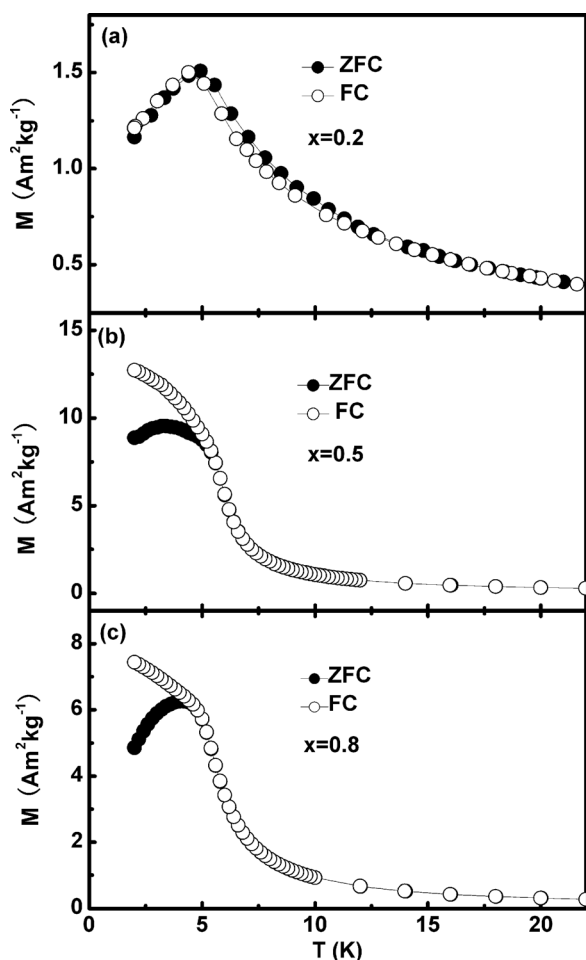


FIG. 1. Temperature dependences of magnetization measured in ZFC and FC modes for $\text{ErNi}_{1-x}\text{Cu}_x\text{Al}$ compounds: (a) $x=0.2$, (b) $x=0.5$, and (c) $x=0.8$.

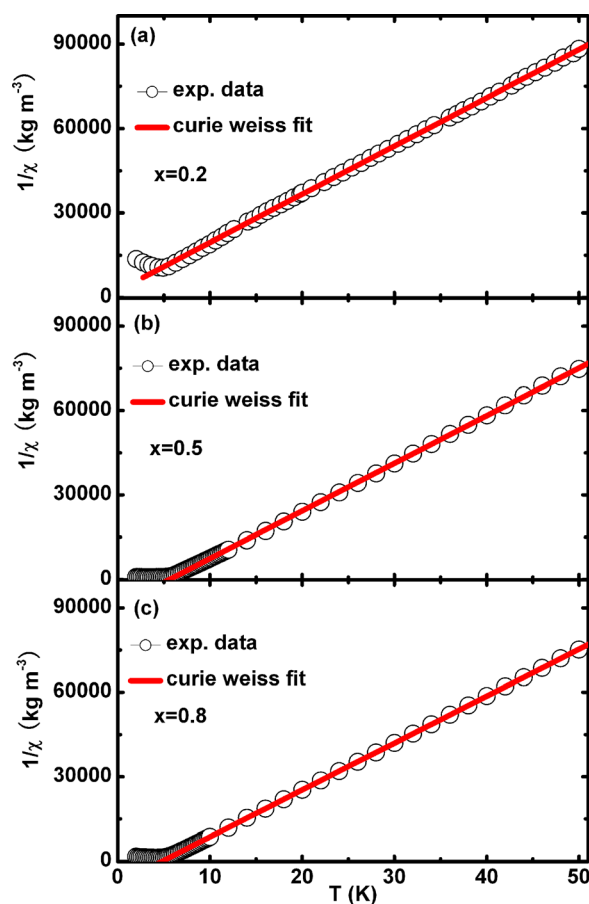


FIG. 2. Temperature variations of the inverse susceptibility fitted to the Curie-Weiss law for $\text{ErNi}_{1-x}\text{Cu}_x\text{Al}$ compounds: (a) $x=0.2$, (b) $x=0.5$, and (c) $x=0.8$.

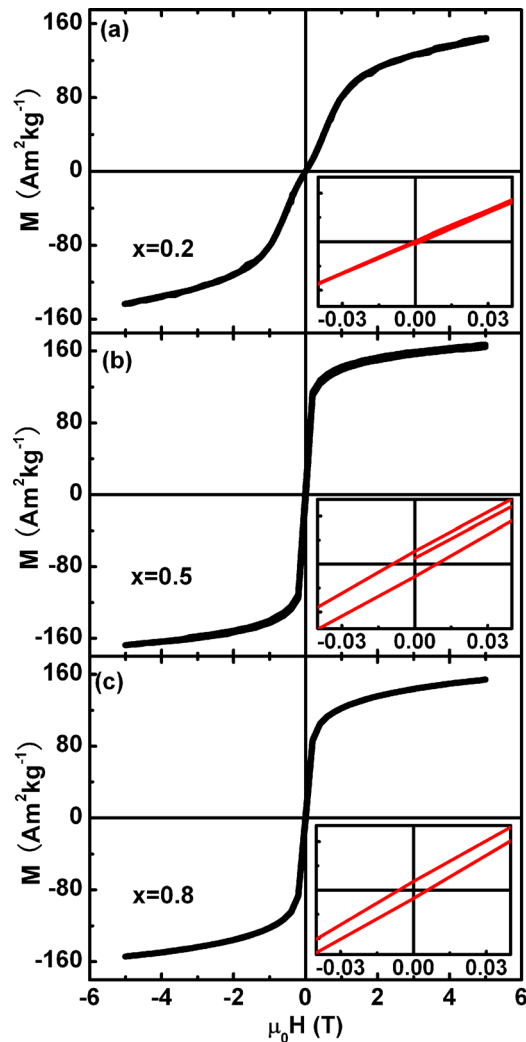


FIG. 3. Magnetic hysteresis loops at 2 K up to 5 T for (a) $x=0.2$, (b) $x=0.5$, and (c) $x=0.8$, respectively, with the insets showing the corresponding coercive fields.

parameters, unusual changes in a are found at 296 K and 15 K for samples $x = 0.6$ and $x = 0.8$, as reported in Ref. 22, which confirms a close relationship between the magnetic ordering and lattice parameters. More work need to be done in the future to identify this scenario. Figure 2 displays the temperature variations of the inverse ZFC susceptibility ($1/\chi$) for $x = 0.2$, $x = 0.5$, and $x = 0.8$, derived from the corresponding $M-T$ curves. One can see that the susceptibilities obey the Curie-Weiss law in the PM regime for all the samples. Further analysis gives the effective magnetic moment (μ_{eff}) of 9.71, 9.72, and $9.9\mu_{\text{B}}/\text{Er}^{3+}$ for $x = 0.2$, $x = 0.5$, and $x = 0.8$, which are slightly larger than the free ion value of Er^{3+} ($9.59\mu_{\text{B}}$). A similar phenomenon has been observed in an isostructural RNiAl compound and was interpreted by the polarization of the conduction band, which is attributed to the magnetic polaronic effect.²⁵ The paramagnetic Curie temperatures (θ_p) obtained are equal to -1.4 , 5.6 , and 4.8 K for the three samples, respectively. The negative value of θ_p indicates the AFM ordering in the $x = 0.2$ sample, whereas the positive value of θ_p indicates the presence of FM order in the $x = 0.5$ and $x = 0.8$ samples. These results coincide with the published

papers.²² In addition, an obvious irreversibility between the ZFC and FC curves are observed at low temperatures for the $x = 0.5$ and $x = 0.8$ samples. Generally speaking, the thermo-magnetic irreversibility is often observed in narrow-domain wall pinning systems and/or frustrated systems. The hexagonal structure in $\text{ErNi}_{1-x}\text{Cu}_x\text{Al}$ coupled with the high anisotropy field or domain wall pinning effect may lead to the irreversibility observed here and this should be verified in the future.^{22,25}

Figures 3(a)–3(c) show the magnetic hysteresis loops at 2 K of the samples with $x = 0.2$, $x = 0.5$, and $x = 0.8$, respectively. Different from the $x = 0.5$ and $x = 0.8$ samples that exhibit FM orderings, an obvious change is detected in the $M-H$ slope at a field of 0.5 T for the $x = 0.2$ sample, implying a phase transition under this field. The insets of Figs. 3(a)–3(c) show the coercive fields of the three samples that are found to be 0, 0.007, and 0.005 T, respectively. In addition, the hysteresis is negligible for all three samples, which is very favorable for the practical application as magnetic refrigerants.

Figures 4(a)–4(f) show the isothermal magnetization curves as a function of magnetic field and the corresponding Arrott-plots (M^2 VS H/M) for $\text{ErNi}_{1-x}\text{Cu}_x\text{Al}$ compounds, measured at various temperatures. It is found that all isotherms show a curvature in the low temperature range, which is a feature of ordered state. It should be noted that some isotherms above T_{ord} also exhibit curvature behaviors that were also observed in Tb_2PdSi_3 and HoNiAl and explained by the magnetic polaronic-like effect attributed to the polarization of the 3d band of Ni.^{25,26} The negative slopes of the Arrott plots below T_N , which are shown in Fig. 4(b) and its inset, indicate the occurrence of a first-order transition for $x = 0.2$, whereas the phase transitions for $x = 0.5$ and $x = 0.8$ as shown in Figs. 4(d) and 4(f) are second-order in nature.²⁷

The long-range order (LRO) in $x = 0.5$ and SRO in $x = 0.8$ sample have been reported by neutron diffraction technique, but the obvious difference between them cannot be identified neither in the $M-T$ curves nor in the $M-H$ curves. In the previous discussion, the discrepancy between ZFC and FC curves has been explained by narrow-domain wall pinning and/or frustrated effects. Taking into account the SRO in the $x = 0.8$ compound, we believe that there may be a tendency toward a glass state if different orders coexist and against each other, preventing the formation of the LRO. The competitions of different mechanisms may induce magnetic frustration or moment freezing. Aiming at obtaining more detailed information about the magnetic properties of the $x = 0.8$ sample and for a comparison between the $x = 0.5$ and $x = 0.8$ samples, we measured the frequency-dependent AC-susceptibilities of these two samples without external DC magnetic field. Figures 5(a) and 5(b) exhibit the real parts of the first order AC magnetic susceptibility for $x = 0.8$ and $x = 0.5$, respectively. The insets of Fig. 5 show the enlarged parts of the graph around the peak position. It is visible in the inset of Fig. 5(a) that the peaks are sharp and shift toward higher temperatures as the frequency increases, which is usually considered as a sign of the existence of glass state. On the contrary, the peaks of $x = 0.5$ sample are broadened and the peak positions are independent of frequency.

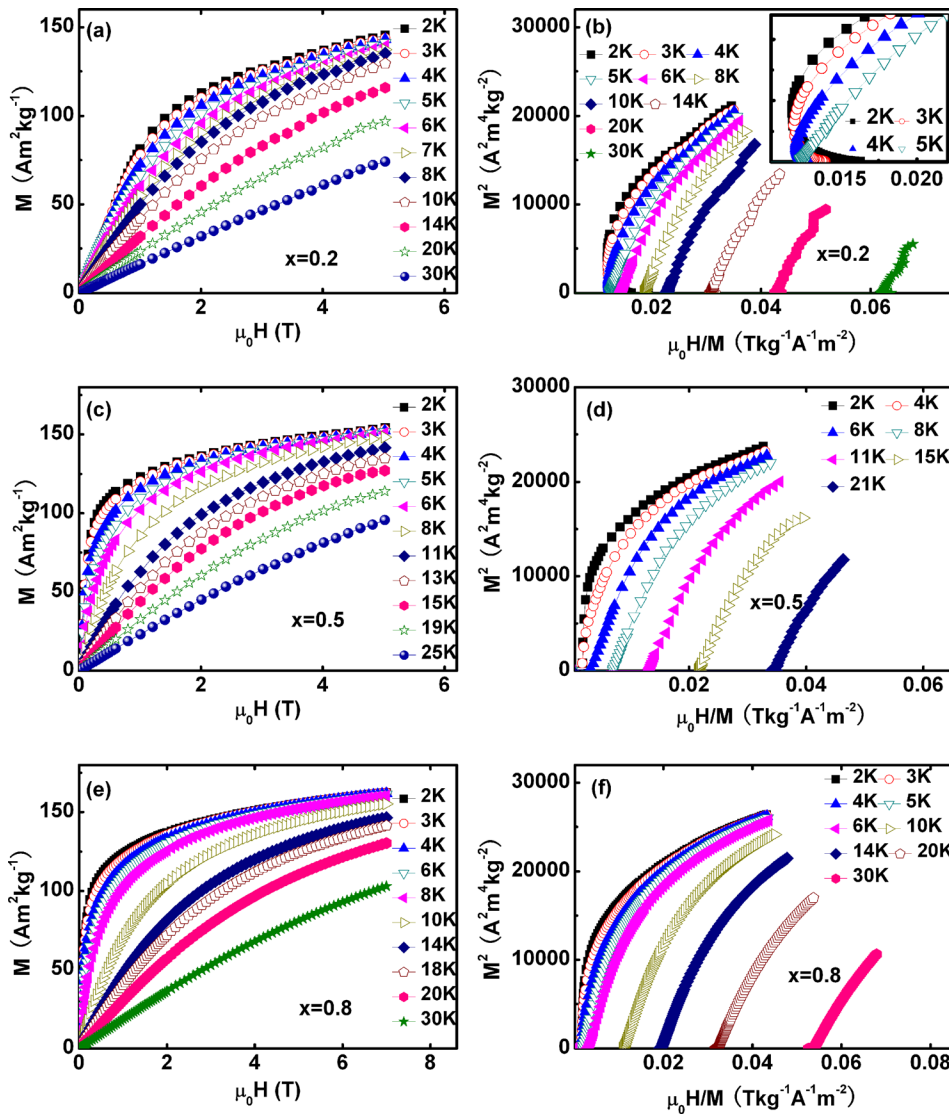


FIG. 4. Magnetic isothermals and Arrott-plots of $\text{ErNi}_{1-x}\text{Cu}_x\text{Al}$ compounds measured during field increasing. The inset of (b) displays the Arrott-plots of $x=0.2$ at typical temperatures.

These results reveal the distinct difference of the magnetism of $x=0.5$ sample and that of $x=0.8$ and can be taken as an identification of the SRO in the $x=0.8$ sample. A similar glass state is also observed in $\text{NdNi}_{1-x}\text{Cu}_x\text{Al}$ sample and be fixed by the AC magnetic measurement.²⁸

The isothermal magnetic entropy change, which is a characterization of the MCE, is determined by Maxwell's relationship $\Delta S = \int_0^H (\partial M / \partial T)_H dH$ in which T is the absolute temperature and H is the applied field. The temperature variations of ΔS for different magnetic field changes are shown in Fig. 6. Different from the other two samples, the sample with $x=0.2$ has positive values of ΔS as shown in Fig. 6(a) and its inset, co-ordinating with the AFM nature of this sample. The ΔS of all samples show peaks between 4 K and 10 K and the maximum values of ΔS are -22.6 , -25.9 , and -24.8 J/kg K for a field change of 0–5 T, respectively. It is evident that the peak values of ΔS are comparable to those of the most promising potential magnetic refrigerant materials in low temperature regime.^{18,29–32} Particularly, it is worthwhile to note that giant ΔS values of -10.1 , -14.7 , and -15.7 J/kg K are achieved for a small field change of 0–2 T, which is promising for practical applications.

We focus not only on the magnitude of the ΔS but also on the refrigerant capacity (RC) that is another important parameter often used to characterize the refrigerant efficiency. In this paper, we use a popular method in Ref. 33 to calculate the value of RC for the $\text{ErNi}_{1-x}\text{Cu}_x\text{Al}$ compounds by numerically integrating the area under the ΔS versus T plot (Fig. 6), over the temperature range determined by the half maximum of the ΔS peak.²⁰ The RC values are 257, 357, and 370 J/kg for a field change of 0–5 T, and 60, 114, and 137 J/kg for 0–2 T. Both sets of RC values are significantly large. For a summary, in Table I, we tabulate the parameters characterizing the magnetic and MCE properties of the $\text{ErNi}_{1-x}\text{Cu}_x\text{Al}$ compounds studied here and the earlier reports.^{28,30,31} The outstanding performances make $\text{ErNi}_{1-x}\text{Cu}_x\text{Al}$ the promising candidates of refrigerant for the magnetic cooling below 10 K.

IV. CONCLUSIONS

In summary, DC and AC magnetic measurement results indicate that $\text{ErNi}_{1-x}\text{Cu}_x\text{Al}$ series with $x=0.2$, $x=0.5$, and $x=0.8$ crystallizing in the ZrNiAl -type structures exhibit

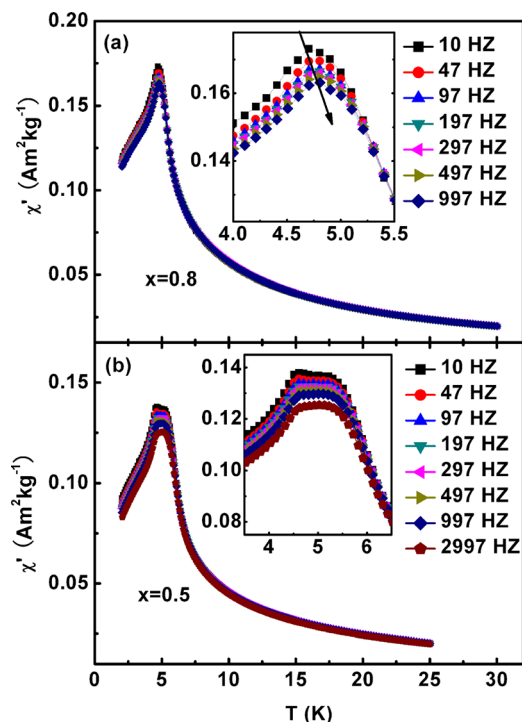


FIG. 5. Temperature dependences of first order (real part) AC magnetic susceptibility for $x = 0.8$ (a); $x = 0.5$ (b). The insets show the corresponding enlarged parts of peak positions at different frequencies.

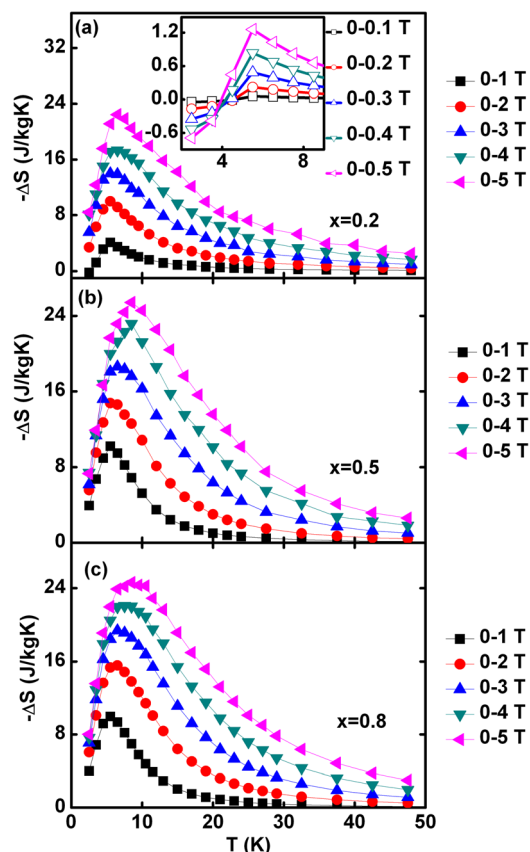


FIG. 6. Magnetic entropy changes as function of temperatures for $\text{ErNi}_{1-x}\text{Cu}_x\text{Al}$ compounds for various magnetic field changes.

TABLE I. Summary of magnetic and MCE properties of $\text{ErNi}_{1-x}\text{Cu}_x\text{Al}$ compounds.

Sample	Type of magnetic ground state	T_{ord} (K)	$-\Delta S$ (J/kg K)		RC(J/kg)	
			(0-2 T)	(0-5 T)	(0-2 T)	(0-5 T)
$X = 0^{30}$	AFM	6		22.3		248
$X = 0.2$	AFM	4.6	10.1	22.6	60	257
$X = 0.4^{28}$	AFM	4	15.5	22.5	122	354
$X = 0.5$	FM	5.8	14.7	25.9	114	357
$X = 0.8$	SRO	5.5	15.7	24.8	137	370
$X = 1^{31}$	FM	7	14.8	22.9	88	321

AFM ordering, FM ordering and SRO, respectively. Their T_{ord} are all lower than 6 K. Large reversible MCE is induced due to the phase transition. For a field change of 0-5 T, the peak values of ΔS are -22.6 , -25.9 , and -24.8 J/kg K for $x = 0.2$, $x = 0.5$, and $x = 0.8$, respectively. Meanwhile, corresponding RC values can reach 257, 357, and 370 J/kg, respectively. The large MCE, high RC, and the magnetic softness jointly make $\text{ErNi}_{1-x}\text{Cu}_x\text{Al}$ compounds favorite candidates for low temperature (< 10 K) magnetic refrigerant.

ACKNOWLEDGMENTS

This work was supported by the National Natural Science Foundation of China (Grant Nos. 11274357, 51021061, and 51271196), the Key Research Program of the Chinese Academy of Sciences, the Hi-Tech Research and Development program of China (Grant No. 2011AA03A404), the National Basic Research Program of China (Grant No. 2010CB833102), and partially the Beijing Excellent talent training support (Grant No. 2012D005016000002).

¹K. A. Gschneidner, Jr., V. K. Pecharsky, and A. O. Tsokol, *Rep. Prog. Phys.* **68**, 1479 (2005).

²E. Brück, in *Handbook of Magnetic Materials*, edited by K. H. J. Buschow (Elsevier B. V., 2008), vol. 17, p. 235.

³B. G. Shen, J. R. Sun, F. X. Hu, H. W. Zhang, and Z. H. Cheng, *Adv. Mater.* **21**, 4545 (2009).

⁴B. G. Shen, F. X. Hu, Q. Y. Dong, and J. R. Sun, *Chin. Phys. B.* **22**, 017502 (2013).

⁵F. Wang, Y. F. Chen, G. J. Wang, J. R. Sun, and B. G. Shen, *Chin. Phys.* **12**, 911 (2003).

⁶F. X. Hu, B. G. Shen, J. R. Sun, and G. H. Wu, *Phys. Rev. B* **64**, 132412 (2001).

⁷O. Tegus, E. Bruck, K. H. J. Buschow, and F. R. de Boer, *Nature (London)* **415**, 150 (2002).

⁸V. K. Pecharsky and K. A. Gschneidner, Jr., *Phys. Rev. Lett.* **78**, 4494 (1997).

⁹F. X. Hu, B. G. Shen, J. R. Sun, and X. X. Zhang, *Chin. Phys.* **9**, 550 (2000).

¹⁰J. A. Barclay and W. A. Steyert, *Cryogenics* **22**, 73 (1982).

¹¹G. J. Liu, J. R. Sun, J. Z. Wang, and B. G. Shen, *Appl. Phys. Lett.* **89**, 222503 (2006).

¹²Y. Y. Zhu, K. Asamoto, Y. Nishimura, T. Kouen, S. Abe, K. Matsumoto, and T. Numazawa, *Cryogenics* **51**, 494 (2011).

¹³J. Jarosz, E. Talik, T. Mydlarz, J. Kusz, H. Böhm, and A. Winiarski, *J. Magn. Magn. Mater.* **208**, 169 (2000).

¹⁴P. Javorský, L. Havela, V. Sechovský, H. Michor, and K. Jurek, *J. Alloys Compd.* **264**, 38 (1998).

¹⁵A. V. Andreev, P. Javorský, and A. Lindbaum, *J. Alloys Compd.* **290**, 10 (1999).

¹⁶P. Javorský, P. Burlet, V. Sechovský, R. R. Arons, E. Ressouche, and G. Lapertot, *Physica B* **234**, 665 (1997).

- ¹⁷P. Javorský, P. Buriak, E. Ressouche, V. Sechovský, and G. Lapertot, *J. Magn. Magn. Mater.* **159**, 324 (1996).
- ¹⁸N. K. Singh, K. G. Suresh, R. Nirmala, A. K. Nigam, and S. K. Malik, *J. Appl. Phys.* **99**, 08K904 (2006).
- ¹⁹H. Takeya, V. K. Pecharsky, K. A. Gschneidner, Jr., and J. O. Moorman, *Appl. Phys. Lett.* **64**, 2739 (1994).
- ²⁰B. J. Korte, V. K. Pecharsky, and K. A. Gschneidner, Jr., *J. Appl. Phys.* **84**, 5677 (1998).
- ²¹J. Prchal, P. Javorský, B. Detlefs, S. Daniš, and O. Isnard, *J. Magn. Magn. Mater.* **310**, e589 (2007).
- ²²J. Prchal, P. Javorský, V. Sechovský, M. Dopita, O. Isnard, and K. Jurek, *J. Magn. Magn. Mater.* **283**, 34 (2004).
- ²³J. Prchal, T. Naka, M. Míšek, O. Isnard, and P. Javorský, *J. Magn. Magn. Mater.* **316**, e499 (2007).
- ²⁴G. Ehlers, D. Ahlert, C. Ritter, W. Miekeley, and H. Maletta, *Europhys. Lett.* **37**(4), 269 (1997).
- ²⁵N. K. Singh, K. G. Suresh, R. Nirmala, A. K. Nigam, and S. K. Malik, *J. Appl. Phys.* **101**, 093904 (2007).
- ²⁶R. Mallik, E. V. Sampathkumaran, and P. L. Paulose, *Solid State Commun.* **106**, 169 (1998).
- ²⁷S. K. Banerjee, *Phys. Lett.* **12**, 16 (1964).
- ²⁸J. Prchal, E. Šantavá, and D. Schmoranzler, *Physica B* **404**, 3056 (2009).
- ²⁹L. C. Wang, Q. Y. Dong, Z. Y. Xu, F. X. Hu, J. R. Sun, and B. G. Shen, *J. Appl. Phys.* **113**, 023916 (2013).
- ³⁰J. kaštil, P. Javorský, and A. V. Andreev, *J. Magn. Magn. Mater.* **321**, 2318 (2009).
- ³¹Q. Y. Dong, J. Chen, J. Shen, J. R. Sun, and B. G. Shen, *J. Magn. Magn. Mater.* **324**, 2676 (2012).
- ³²X. X. Zhang, F. W. Wang, and G. H. Wen, *J. Phys.: Condens. Matter* **13**, L747 (2001).
- ³³K. A. Gschneidner, Jr., V. K. Pecharsky, A. O. Pecharsky, and C. B. Zimm, *Mater. Sci. Forum* **69**, 315 (1999).